Tuning of optical resonances in asymmetric microtube cavities

Libo Ma,[1] Suwit Kiravittaya,[1] Vladimir A. Bolaños Quiñones,[1] Shilong Li,[1] Yongfeng Mei,[3,*] and Oliver G. Schmidt[1,2]

[1]*Institute for Integrative Nanosciences, Leibniz-Institut für Festkörper-und Werkstoffforschung Dresden, Helmholtzstrasse 20, D-01069 Dresden, Germany*

[2]*Material Systems for Nanoelectronics, Chemnitz University of Technology, Reichenhainer Strasse 70, D-09107 Chemnitz, Germany*

[3]*Department of Materials Science, Fudan University, Handan Road 220, Shanghai 200433, China*

**Corresponding author: yfm@fudan.edu.cn*

Received August 22, 2011; accepted August 31, 2011;
posted September 7, 2011 (Doc. ID 153203); published September 26, 2011

We tune optical resonances in rolled-up SiO/SiO_2 microtube cavities by gradually modifying the tube structure through asymmetrical postdeposition of SiO_2. Spectral blueshifts followed by redshifts of the resonant modes are observed in a thin-walled microtube (tube-I), which is attributed to a competition between shape deformation and effective increase of tube wall thickness. In contrast, only a monotonic redshift is detected when asymmetrical deposition is performed on a thick-walled microtube (tube-II). Distinct wavelength-dependent tuning was revealed in both kinds of tubes. Numerical calculations based on perturbation theory are carried out to explain and confirm the experimental results.

OCIS codes: 230.5750, 140.3945, 260.5740, 310.6628, 060.4080.

Conventional circular structures such as microspheres [1], microdisks [2], and microrings [3] are often selected to serve as optical cavities, in which light resonates as whispering-gallery modes by total internal reflection. Among those cavities, planar microrings possess promising potential for all-optical circuits, such as optical wavelength switches/converters [4,5], add–drop filters [6], and notch filters [7]. Rolled-up microtubes, novel to our knowledge, are vertical ringlike optical cavities [8,9]. Recently, photonic devices such as wavelength-tunable emitters [10], microtube lasers [11], and passive filters [12] have been realized by using GaAs-based microtubes as core components. Other interesting aspects and phenomena, such as directional light emission [13] and enhanced coupling of ring resonators [14], might be feasible by deliberately introducing asymmetry into the structure.

In this Letter, we tune optical resonances by stepwise deposition of SiO_2 onto SiO/SiO_2-based microtube cavities. These microtubes are prepared by releasing prestrained SiO/SiO_2 bilayers on Si substrate using the technique reported in our previous studies [15–17]. For the cavity modification, the microtubes are introduced into an electron-beam evaporation chamber, where SiO_2 is deposited on the tube wall. During the deposition, the depositing beam is perpendicular to the substrate surface; therefore, the SiO_2 is only grown on the top side of the microtubes, which are fully integrated on the substrate. In this way the microtube cavities are asymmetrically modified. The final shape of the modified tube cross section consists of a ring and an SiO_2 nanocap on the top side. After each SiO_2-deposition step, the light emission spectra are measured at room temperature using a conventional confocal microphotoluminescence (μ-PL) setup with an He–Cd laser line at 442 nm as an excitation source. During the μ-PL measurement, the laser optically excites Si nanoclusters, which are embedded in the oxide layers [18]. The PL emission from these nanoclusters provides light for the resonances in the tube microcavity. Optical resonant modes are formed by constructive interference of light circulating in the tube wall [16].

Two kinds of microtubes are prepared for the resonance tuning. Tube-I has a wall thickness of ~189 nm and a tube diameter of ~5.9 μm as a relatively flexible structure. Tube-II has a wall thickness of ~344 nm and a diameter of ~3.7 μm as a relatively rigid structure. In addition, the inner and outer tube wall surfaces of tube-II were coated with a 30 nm HfO_2 layer by atomic layer deposition (ALD) to further strengthen the tube structure. The asymmetric modifications of the microtube cavities by SiO_2 deposition are schematically shown in Figs. 1(a) and 2(a) for tube-I and tube-II, respectively. Figure 1(b) shows the PL spectra of tube-I after a series of SiO_2 depositions. The optical resonant modes are

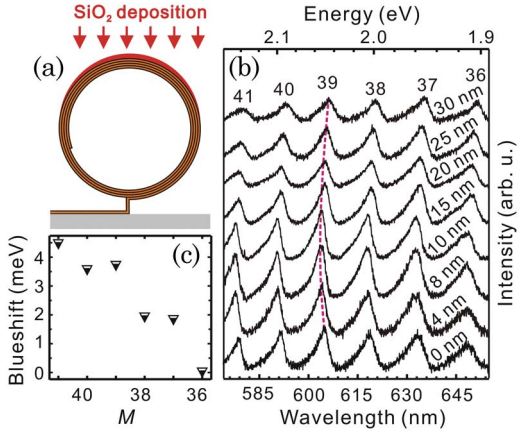

Fig. 1. (Color online) (a) Sketch of tube-I cross section during SiO_2 deposition. (b) PL spectra of tube-I after a series of SiO_2 nanocap depositions (from bottom to top: 0, 4, 8, 10, 15, 20, 25, and 30 nm). The resonant modes are labeled with the calculated azimuthal mode number M. Evolution of mode position at $M = 39$ is guided by a dashed line. (c) Maximum mode blueshift as a function of M.

evident from the distinct peaks with a free spectral range (FSR) of around 45 meV and are defined as TM modes, which have electric field linearly polarized along the tube axis [17]. Every mode in the spectrum is labeled with the corresponding azimuthal mode number M, calculated under resonance condition [16]. Up to the first 8 nm SiO_2 deposited, the resonant modes only show blueshifts, whereas the modes turn to a redshift when further SiO_2 is deposited. Figure 1(c) represents the blueshifts of resonant modes at different M when 8 nm thick SiO_2 is deposited. The blueshift (ΔE) decreases for the modes at shorter wavelengths (e.g., $\Delta E = 4.5$ meV at $M = 41$) to the longer wavelength modes (e.g., $\Delta E \sim 0$ meV at $M = 36$). Within the range of our SiO_2 deposition, the total observed mode shift ($E_{max} - E_{min}$, where E_{max} and E_{min} are the maximum and minimum position during the mode shift, respectively) is 11.2 meV for mode $M = 41$ and decreases to 9.3 meV for mode $M = 36$. Furthermore, we also notice that the Q factor can be tuned by SiO_2 deposition and it shows a wavelength-dependent behavior. During the increase of the SiO_2 nanocap thickness, the Q factor continuously decreases for modes at shorter wavelength (see mode $M = 41$), while the Q factor firstly increases and then decreases for the modes at longer wavelength. Since the tube wall thickness (~189 nm) is three times smaller than the resonant wavelength (570–660 nm), the light confinement will be substantially improved by the effectively increased wall thickness due to the presence of the SiO_2 nanocap. At the same time, the microcavity becomes more asymmetric after each SiO_2-deposition step. As a result, the light losses might be enhanced by taper loss [19], which is induced by the nonuniformity of the wall thickness due to the postdeposited nanocap. The competition between better confinement and enhanced light losses is responsible for the evolution of the Q factor.

Figure 2(b) shows the PL spectra of tube-II with an FSR of around 55 meV after a series of SiO_2 depositions. Contrary to tube-I, exclusively redshifts of the resonant

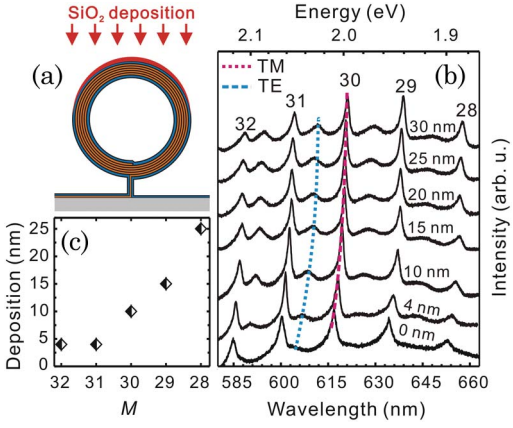

Fig. 2. (Color online) (a) Sketch of tube-II cross section during SiO_2 deposition. (b) PL spectra of tube-II after a series of SiO_2 nanocap depositions (from bottom to top: 0, 4, 10, 15, 20, 25, and 30 nm). TM modes are labeled with the calculated azimuthal mode number M. Evolution of TM mode position at $M = 30$ is guided by a dashed line. TE modes gradually appear as the SiO_2 nanocap thickness is increased. Evolution of a TE mode is marked by a dotted line. (c) Thickness of deposited SiO_2 nanocap at the maximum Q factor as a function of M.

modes are observed after SiO_2 deposition, but the wavelength-dependent mode tuning remains. After 30 nm thick SiO_2, the mode shift is 13.4 meV for $M = 32$, and the shift increases to 14.1 meV for mode $M = 28$. Moreover, additional peaks emerge along with resonant TM mode peaks. These new resonant mode peaks are TE modes [17] with electric field vectors perpendicular to the tube axis. The thicker tube wall in this microtube (tube-II) contributes to the presence of TE modes, which was previously reported for ALD coating of Al_2O_3 layers on microtube cavities [17]. This explanation is supported by the fact that the intensities of TE modes increase after depositing thicker SiO_2 nanocaps, as shown in Fig. 2(b). Figure 2(c) shows the thicknesses of the SiO_2 nanocaps providing the maximum observed Q factors for different M. After deposition of 4 nm thick SiO_2 nanocaps, the maximum Q factors are observed for shorter-wavelength modes (M: 31, 32). When further SiO_2 is deposited, the Q factors tend to decrease due to the enhanced light losses, as we discussed before. It is found that a thicker SiO_2 nanocap is required for obtaining maximum Q at longer wavelengths; e.g., the Q factor of mode $M = 28$ (at ~657 nm) reaches a maximum for a 25 nm thick SiO_2 nanocap.

Resonant wavelengths in the geometry-modified microtube cavities are calculated using a two-dimensional ring resonator model and perturbation theory [20]. Since the structural change is in the nanometer range and therefore small compared to the tube diameter, perturbation theory is a suitable tool to calculate the mode shifts. It is conceivable that the resonant mode will redshift if a nanocap is introduced to a microcavity. However, considering the fairly thin tube wall of tube-I, an oval-shape deformation induced by SiO_2 deposition, which is illustrated in the lower-right inset of Fig. 3(a), is suggested to explain the blueshift of the resonant modes. The shape-deformation-induced blueshift was also confirmed by directly pressing the microtube with a capillary tip, which was not shown here. Furthermore, a blueshift caused by shape deformation was also observed in a study of elliptic microdisk resonators [21]. The calculation results are in agreement with the experimental results on different M. Here we select mode $M = 39$ for tube-I and $M = 31$ for tube-II as examples to discuss different tuning mechanisms. When only considering the presence of the SiO_2 nanocap, which effectively increases the tube wall thickness, the calculations clearly indicate a redshift of the resonant mode, as shown in Fig. 3. When the cavity is deformed from circular to oval geometry, a blueshift is obtained as a function of cavity deformation [21], as shown in the upper-left inset of Fig. 3(a). The competition between shape deformation and effective increase of the tube wall thickness results in blueshifts followed by redshifts of the resonant mode in tube-I. Considering the mode shifts induced by both the shape deformation (D) and the postdeposited SiO_2 nanocap, a shape deformation $D = 36.2$ nm of the cavity structure is estimated when an 8 nm thick SiO_2 cap is deposited on tube-I. Resonant modes in tube-II do not show any blueshift after SiO_2 deposition, which can be understood bearing in mind that tube-II has a thicker tube wall and smaller diameter compared to those of tube-I. In addition, tube-II is strengthened by a 30 nm HfO_2 layer.

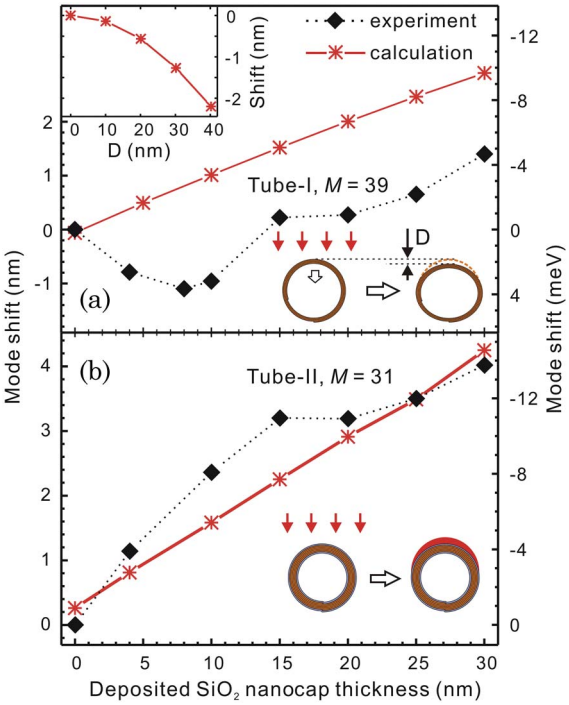

Fig. 3. (Color online) (a) Experimental (diamonds) and calculated (asterisks) mode shift for the mode $M = 39$ in tube-I. Post-deposited SiO_2 nanocap leads to redshift. Cavity deformation (D) results in blueshift, as shown in upper-left inset. Lower-right inset shows the definition of D. (b) Experimental (diamonds) and calculated (asterisks) mode shift for the mode $M = 31$ in tube-II with only SiO_2 nanocap considered.

Hence, the tube structure is robust enough to prevent any shape deformation during SiO_2 deposition.

In conclusion, we have explored a simple method to manufacture asymmetric resonant cavities, in which the optical resonances are tuned by gradually changing the geometry of microtube cavities through SiO_2 depositions. Calculations of optical resonances are performed by using a two-dimensional ring resonator model and perturbation theory, where the effects of SiO_2 nanocaps and/or shape deformations are considered. We demonstrate that the cavity deformation is responsible for the blueshift, while the presence of nanocaps leads to the redshift of resonant modes. This finding implies a way to detect small shape deformation in a microcavity. The wavelength-dependent resonance tuning opens a way to simultaneously tune different modes in one optical microtube cavity. Furthermore, the high optical sensitivity for small perturbations on the microcavity offers a possible implementation of an efficient sensing function of the microtube resonators.

The authors thank R. Engelhard for technical assistance. This work was financially supported by the Volkswagen Foundation (I/84072) and the United States Air Force Office of Scientific Research (USAFOSR) Multidisciplinary University Research Initiative (MURI) program under grant FA9550-09-1-0550. Y.-F. Mei thanks the support from the National Natural Science Foundation of China (NSFC) (61008029), the Program for New Century Excellent Talents in University (NCET-10-0345), and the Shanghai Pujiang Program (11PJ1400900). S.-L. Li thanks the financial support from China Scholarship Council (CSC). L.-B. Ma thanks the support from grants KGCX2-YW-360, 10974227, and 60621091 by the Chinese Academy of Sciences (CAS).

References

1. M. L. Gorodetsky, A. A. Savchenkov, and V. S. Ilchenko, Opt. Lett. **21**, 453 (1996).
2. S. L. McCall, A. F. J. Levi, R. E. Slusher, S. J. Pearton, and R. A. Logan, Appl. Phys. Lett. **60**, 289 (1992).
3. J. K. Poon, L. Zhu, G. A. DeRose, and A. Yariv, Opt. Lett. **31**, 456 (2006).
4. V. R. Almeida, C. A. Barrios, R. R. Panepucci, and M. Lipson, Nature **431**, 1081 (2004).
5. Q. Xu, V. R. Almeida, and M. Lipson, Opt. Lett. **30**, 2733 (2005).
6. S. T. Chu, B. E. Little, W. Pan, T. Kaneko, and J. Kokubun, IEEE Photon. Technol. Lett. **11**, 1423 (1999).
7. P. P. Absil, J. V. Hryniewicz, B. E. Little, R. A. Wilson, L. G. Joneckis, and P. T. Ho, IEEE Photon. Technol. Lett. **12**, 398 (2000).
8. T. Kipp, H. Welsch, Ch. Strelow, Ch. Heyn, and D. Heitmann, Phys. Rev. Lett. **96**, 077403 (2006).
9. R. Songmuang, A. Rastelli, S. Mendach, and O. G. Schmidt, Appl. Phys. Lett. **90**, 091905 (2007).
10. S. Mendach, S. Kiravittaya, A. Rastelli, M. Benyoucef, R. Songmuang, and O. G. Schmidt, Phys. Rev. B **78**, 035317 (2008).
11. Ch. Strelow, M. Sauer, S. Fehringer, T. Korn, C. Schüller, A. Stemmann, Ch. Heyn, D. Heitmann, and T. Kipp, Appl. Phys. Lett. **95**, 221115 (2009).
12. Z. B. Tian, V. Veerasubramanian, P. Bianucci, S. Mukherjee, Z. T. Mi, A. G. Kirk, and D. V. Plant, Opt. Express **19**, 12164 (2011).
13. K. Shima, R. Omori, and A. Suzuki, Opt. Lett. **26**, 795 (2001).
14. P. P. Absil, J. V. Hryniewicz, B. E. Little, P. S. Cho, R. A. Wilson, L. G. Joneckis, and P.-T. Ho, Opt. Lett. **25**, 554 (2000).
15. Y. F. Mei, G. S. Huang, A. A. Solovev, E. Bermúdez Ureña, I. Mönch, F. Ding, R. Reindl, R. K. Y. Fu, P. K. Chu, and O. G. Schmidt, Adv. Mater. **20**, 4085 (2008).
16. G. S. Huang, S. Kiravittaya, V. A. Bolaños Quiñones, F. Ding, M. Benyoucef, A. Rastelli, Y. F. Mei, and O. G. Schmidt, Appl. Phys. Lett. **94**, 141901 (2009).
17. V. A. Bolaños Quiñones, G. S. Huang, J. D. Plumhof, S. Kiravittaya, A. Rastelli, Y. F. Mei, and O. G. Schmidt, Opt. Lett. **34**, 2345 (2009).
18. L. X. Yi, J. Heitmann, R. Scholz, and M. Zacharias, Appl. Phys. Lett. **81**, 4248 (2002).
19. A. Shahar, W. J. Tomlinson, A. Yi-Yan, M. Seto, and R. J. Deri, Appl. Phys. Lett. **56**, 1098 (1990).
20. S. G. Johnson, M. Ibanescu, M. A. Skorobogatiy, O. Weisberg, J. D. Joannopoulos, and Y. Fink, Phys. Rev. E **65**, 066611 (2002).
21. S. V. Boriskina, T. M. Benson, P. Sewell, and A. I. Nosich, J. Lightwave Technol. **21**, 1987 (2003).